Atomistic modeling of amorphous silicon carbide: an approximate first-principles study in constrained solution space



2009 J. Phys.: Condens. Matter 21 265801

(http://iopscience.iop.org/0953-8984/21/26/265801)

J. Phys.: Condens. Matter **21** (2009) 265801 (9pp) doi:10.1088/0953-8984/21/26/265801

# Atomistic modeling of amorphous silicon carbide: an approximate first-principles study in constrained solution space

**Raymond Atta-Fynn**[1] **and Parthapratim Biswas**[2]

[1] Department of Physics and Astronomy, The University of Texas, Arlington, TX 76019, USA
[2] Department of Physics and Astronomy, The University of Southern Mississippi, Hattiesburg, MS 39406, USA

E-mail: attafynn@uta.edu and partha.biswas@usm.edu

Received 18 February 2009, in final form 5 May 2009
Published 3 June 2009
Online at stacks.iop.org/JPhysCM/21/265801

**Abstract**

Localized basis *ab initio* molecular dynamics simulation within the density functional framework has been used to generate realistic configurations of amorphous silicon carbide (a-SiC). Our approach consists of constructing a set of smart initial configurations that conform to essential geometrical and structural aspects of the materials obtained from experimental data, which is subsequently driven via a first-principles force field to obtain the best solution in a reduced solution space. A combination of *a priori* information (primarily structural and topological) along with the *ab initio* optimization of the total energy makes it possible to model a large system size (1000 atoms) without compromising the quantum mechanical accuracy of the force field to describe the complex bonding chemistry of Si and C. The structural, electronic and vibrational properties of the models have been studied and compared to existing theoretical models and available data from experiments. We demonstrate that the approach is capable of producing large, realistic configurations of a-SiC from first-principles simulation that display its excellent structural and electronic properties. Our study reveals the presence of predominant short range order in the material originating from heteronuclear Si–C bonds with a coordination defect concentration as small as 5% and a chemical disorder parameter of about 8%.

(Some figures in this article are in colour only in the electronic version)

## 1. Introduction

Silicon carbide is a wide bandgap semiconductor having a range of applications from optoelectronic devices, gas turbines and heat exchangers to ceramic fans. The amorphous form of SiC is particularly interesting due to the temperature stability of its semiconducting properties, making it possible to use it under extreme condition in applications such as high-temperature engines, turbines and reactors [1–7]. There have been a number of studies of amorphous SiC in recent years with the emphasis mostly on the structural aspect of the material. Of particular importance is the nature of the short range order (SRO) in the material. Despite numerous experimental and theoretical studies, the exact nature of the SRO and the extent of its presence are still unknown. While bonding in its various crystalline counterpart is $sp^3$ corresponding to heteronuclear Si–C bonds, the nature of the bonding chemistry in *a*-SiC is far more complex and is not well understood. Different experimental probes on *a*-SiC often appear to suggest contradictory results: from the presence of purely heteronuclear Si–C bonding to an admixture of heteronuclear Si–C (chemical order) and homonuclear Si–Si and C–C bonds (chemical disorder). Unlike silicon that conforms primarily to tetrahedral $sp^3$ bonding, the complex carbon chemistry permits the atom to hybridize via sp, $sp^2$ and $sp^3$ bond formation in an amorphous environment. The structure of the material also depends on the growth conditions and the subsequent treatment of the sample. As a result, various experimental probes often provide a very different microscopic picture of the material.

In this paper we study the structural, electronic and vibrational properties of a 1000-atom model of *a*-SiC via

 

*ab initio* molecular dynamic simulation using a localized basis set and pseudopotential density functional approach. Our emphasis is on developing an effective approach that models a sufficiently large system size without compromising the accuracy of the interaction among the atoms by focusing on the relevant part of the configuration space by using a suitable prior from experimental data. This has been achieved by generating a set of smart generic configurations and optimizing the resulting structural models in the reduced solution space of the first-principles force field. The paper is organized as follows. In section 2, we provide a brief discussion of earlier works and the present state of knowledge of the material in the amorphous state. Section 3 describes the essential idea behind our method and how to construct smart configurations using experimental information and some geometrical, topological and structural characteristics of the material. The simulation procedure is outlined in section 4, which is then followed by a discussion of the results in section 5.

## 2. Summary of earlier works

There has been a wealth of experimental information available from a range of studies including Raman scattering, electron and x-ray diffraction to Auger spectroscopy; however, none of these studies can provide a conclusive picture of the structural properties of the material in the amorphous state. A number of experimental studies (such as Raman scattering [8] and x-ray diffraction [9]) have indicated a significant presence of chemical disorder via homonuclear bond formation, whereas there is evidence from Auger [10], x-ray photoemission [11] and extended x-ray absorption [12] experiments indicating the presence of heteronuclear bonds. Kaloyeros *et al* [12] performed extended x-ray absorption spectra and energy loss fine structure experiments to study sputtered *a*-SiC films and concluded that the short range chemical order essentially consisted of only Si–C heteronuclear bonds. An x-ray adsorption and Raman spectroscopy study by Bolse [13] of SiC amorphized by ion bombardment concluded that the chemical short range order not only comprised Si–C bonds but also homonuclear C–C and Si–Si bonds. Electron diffraction studies of SiC amorphized by ion beams confirms this observation [9], and shows the recovery of the SRO upon annealing to 1073 K [14]. Fast neutron irradiation induced amorphization of SiC experiments by Snead *et al* revealed that the atomic density of *a*-SiC 2.85 g cm$^{-3}$ at 300 K increased to 3 g cm$^{-3}$ after annealing at 1100 K due to the recovery of SRO [15]. The picture that emerges from these experimental results points to the fact that *a*-SiC consists of both homo- and heteronuclear bonds, but it is difficult to quantify to what extent the short range chemical ordering is present in the network.

As far as theoretical studies are concerned, a fair amount of work can be found in the literature [16–27]. Finocchi *et al* [16] were the first to perform a quench-from-the-melt *ab initio* molecular dynamics study using 54- and 64-atom supercells and observed that 45% of the total bonds formed by C were homonuclear, of which 15% of the bonds were 3-fold coordinated (sp$^2$) with bond angles close to 120° (making these regions essentially graphite-like) and that *a*-SiC had negligible chemical ordering. A subsequent study by Kelires [17] via quench-from-the-melt Monte Carlo simulations of a 216-atom *a*-SiC sample using the empirical Tersoff potential [18] observed strong chemical ordering, but 50% of the C atoms were 3-fold coordinated and 33% of the C bonds were homonuclear. In an attempt to resolve the discrepancy, Tersoff [19] performed classical MD simulations using an improved version of the empirical potential [18] introducing a measure of chemical disorder via the ratio

$$\chi = \frac{n_{\mathrm{CC}}}{n_{\mathrm{SiC}}}, \tag{1}$$

where $n_{\mathrm{CC}}$ is the number of C–C bonds and $n_{\mathrm{SiC}}$ is the number of Si–C bonds. The value $\chi = 0$ implies no chemical disorder, whereas $\chi = 1$ indicates complete disorder in the network. Based on this definition, the author concluded that if the graphite-like regions in [16] were excluded then the combined results in [16], [17] and [19] corresponded to $0.5 \leqslant \chi \leqslant 0.6$. Mura *et al* [20] performed classical MD simulations for *a*-$Si_xC_{1-x}$ alloys in the composition range $0.125 < x < 0.875$ using the modified Tersoff potential and a 512-atom supercell. For *a*-$Si_{0.5}C_{0.5}$ they obtained $\chi = 0.6$ and concluded that for high C contents the value of $\chi$ is linked to a sizable distortion of the Si sublattice. Ivashchenko *et al* [21] performed sp$^3$s$^*$ tight-binding MD simulations for models of *a*-SiC containing 54–216 atoms. They observed the presence of homonuclear bonds and coordination defect concentration ranges from 6% to 13%. Molecular dynamics (MD) simulations of ion or neutron bombardment of *a*-SiC have been performed by Gao and Weber [22] and by Malerba and Perlado [23]. The former work [22] used the Tersoff potential [19] and obtained $\chi = 0.41$ in the damaged region created by 10 keV Au recoils in a 250 000-atom supercell of 3C-SiC. Similarly, using classical MD simulations and a different version of the Tersoff potential [18], Malerba and Perlado [23] studied the damage accumulation process for 100 eV recoils in a 512-atom supercell of 3C-SiC embedded in a larger bounding crystal containing 1216 atoms. They obtained $\chi = 0.34$ for both the irradiated *a*-SiC and the reference quench-from-the-melt model of a-SiC. However, $\chi$ reduced to 0.22 in the irradiated model and remained at 0.34 for the reference quench-from-the-melt model. Since previous simulations using the Tersoff potential [17, 19] produced $\chi = 0.5$–$0.6$, the rather different results ($\chi = 0.22$–$0.34$) of Malerba and Perlado [23] obtained using the same potential as described above is quite puzzling. However, Yuan and Hobbs have shown that if the amorphous–crystalline boundary is excluded, then the results of Malerba and Perlado [23] will correspond to ($\chi = 0.35$–$0.5$). Quite recently, Devanathan *et al* [25] have performed classical MD simulations using a Brenner-type interatomic potential [26] to model the 4096-atom configuration of a-SiC. They observed that the density of the quenched liquid was in excellent agreement with experiment and $\chi = 0.06$–$0.13$ for annealing temperatures ranging from 300 to 2500 K. Finally, Rino *et al* [27], using an empirical potential with Coulomb, charge-dipole and van der Waals interactions included in the two-body term, performed classical MD simulation for a large supercell of *a*-SiC containing 10 648 atoms and obtained $\chi = 0$, in perfect agreement with the experiments by Kaloyeros *et al* [12].

In summary, the bulk of the experimental and theoretical studies appear to favor a non-zero value of $\chi$ with the exception of the experimental work by Kaloyeros *et al* [12] and the theoretical models proposed by Rino *et al* [27]. As mentioned before, experimental results indicate that bonding in amorphous SiC is a mixture of both homonuclear and heteronuclear bonding consisting of $sp^2$ and $sp^3$ hybridizations. Given the complex nature of bonding chemistry in the amorphous environment, it is not surprising that models based on empirical or semi-empirical potentials are at best incomplete for describing some of the structural and electronic properties of a-SiC. Since most of the theoretical models proposed so far are based on either empirical or semi-empirical potentials, it is important to carry a full-scale first-principles study of *a*-SiC so that the details of the quantum mechanical nature of the bonding between C and Si and the local chemistry can be taken into account in the model construction. While the models proposed by Finocchi *et al* [16] did take into account the quantum mechanical interactions within the density functional theory via the local density approximation, the size of the simulation cell (typically 64 atoms) was too small to realistically represent the properties of bulk a-SiC. Since structural properties are directly linked with the electronic and vibrational properties of the materials, predictive structural modeling should be done in conjunction with calculations of electronic and vibrational properties for a reasonable system size, and to be compared with experiments. Finally, there are very few models in the literature that address the electronic properties of a-SiC [16, 21]. The present study attempts to provide a comprehensive picture of the structural and electronic properties of *a*-SiC by selectively sampling the solution space using the prior information obtained from experiments.

## 3. Strategy of our approximate simulation: sampling solution space with prior information

In conventional electronic structure problems one begins with a set of atomic coordinates and an interacting potential or Hamiltonian. The electronic density of states is obtained either by solving the Schrödinger equation within the first-principles density functional formalism or by constructing a semi-empirical Hamiltonian to compute the electronic eigenstates, total energy and response functions to compare with experiments [28]. For amorphous materials, however, such an approach brings only limited success. The determination of a ground state configuration (or an approximated one) of a glassy system involves identification of the global (or a low lying local) minimum in the multidimensional energy landscape, which is a very difficult problem in computational sciences. The complexity of the problem increases enormously with the increase of system size, and can be solved for a few simple potentials under very restricted conditions [29]. The brute force applications of a first-principles energy functional to model large amorphous systems is not only hopelessly difficult, but also very uninspiring and time-consuming. Most of the *ab initio* methods asymptotically scale as $O(n^3)$ or even faster and seriously constrain the size of the simulation cell and total time to be studied. The so-called order-*N* counterpart of such approaches can improve the situation; however, for disordered materials the use of such methods is frankly very risky. The latter approach exploits the locality of quantum mechanics either via the short range nature of Wannier functions or truncation of density matrix of the system, but such requirements are rarely satisfied at the beginning of simulation for an arbitrary starting configuration. The prohibitive scaling constrains the system to evolve only for a limited time, preventing it from exploring the full solution space. Except for small system size and for a few good glass formers, direct *ab initio* calculations tend to produce unrealistic configurations of the material, and the situation is particularly exacerbated for (amorphous) materials that do not display glassy characteristics [30] (e.g. amorphous silicon).

In recent years there have been a number of methods that make use of the available knowledge of the materials (either experimental or otherwise) in the simulation methodology. These 'knowledge-oriented' approaches have been developed under the general class of techniques based on the information paradigm. Under this wing, one combines the power of a first-principles force field with the available information for the material under study. The general strategy is to construct a series of guesses of the solution that are consistent with experimental observation, and to improve the solution either deterministically or stochastically via an appropriate force field. Examples of methods that are currently in use include 'Decorate-and-Relax' [31], 'Block-MD' [32] and 'Experimentally constrained molecular relaxation (ECMR)' [33], where prior knowledge of the materials is used to accelerate the search procedure for finding a better minimum in the simulation methodology. The imposition of a suitably constructed prior (information) reduces the volume of the search space by hierarchically constructing a more probable solution space, and the system is driven to find the best solution in this subspace. Since the system spends most of its time in the favorable subspace of the desired solutions, it is computationally more efficient and it is likely to find a better estimate of the global minimum of the problem. The essential idea is to 'throw out' the irrelevant part of the solution space by judicious choice of constraints and experimental data available for the material. While there exists no general scheme for guessing a series of candidate solutions for a complex multinary system, one can nonetheless construct a set of disordered networks that shares some of the characteristic features of the material (here a-SiC) obtained from experiments. This is done by introducing various priors in the network, which identify and sample the more probable part of the solution space associated with those priors.

Following this strategy, the starting point of our calculation is to build a series of binary random networks having some degree of local tetrahedral order. Each of the binary networks is then given a different geometrical and topological character by changing the bond lengths, bond angles, atomic coordinations and ring geometry. From a macroscopic point of view, all of these structures have an almost identical tetrahedral character (of varying degree), but topologically they are quite different. A number of samples are

generated with varying degrees of chemical and topological disorder, so that during the course of simulation the system has access to the entire solution subspace of approximated tetrahedral ordering. This particular choice of ordering is motivated by the available experimental data from *a*-SiC (such as the structure factor and bond angle distribution) suggesting the presence of significant tetrahedral-like ordering in the material. It is to be noted that the topological character of this local ordering is very different from the randomized c-SiC structure[3], which is often used as a starting configuration without much thought. While an unbiased, completely random configuration would ideally be the best choice to build models during the course of simulation, such a choice requires one to explore a vast amount of solution space at the expense of computation time without the guarantee of identifying the correct minimum from the potentially correct solution set. The latter approach can be made feasible for identifying the global minimum in small systems (such as clusters, macromolecules and some glasses) [34], but for large systems the number of solutions diverges rapidly with system size. In the present work, the binary random networks are generated via the modified WWW [35] algorithm as proposed by Barkema and Mousseau [36, 37]. The structural and topological properties of these binary networks are further modified so that the resulting networks span the subspace of the entire solution space that are consistent with available experimental data. In particular, we focus here on a 1000-atom model with 50–50 concentration of Si and C having the same density as the experimental atomic density of crystalline 3C-SiC.

## 4. Molecular dynamics simulation procedure

In this work we have used the *ab initio* program SIESTA [38–40], which is capable of determining the electronic structure and properties of molecules, surfaces and bulk materials based on density functional theory (DFT). The Perdew–Zunger formulation of the local density approximation (LDA) is employed [41] along with the norm-conserving Troullier–Martins pseudopotentials [42] factorized in the Kleinman–Bylander form [43] to remove the core electrons. To describe the valence electrons, a set of atomic orbital bases is used that consists of finite range numerical pseudoatomic wavefunctions of the form proposed by Sankey and Niklewski [44]. We employ a single-$\zeta$ (SZ) basis set for all the atoms (one s and three p orbitals per atom) for the present calculation. Although some tight-binding calculations have indicated the need for an improved basis set beyond single-$\zeta$, in this work we restrict ourselves to a single-$\zeta$ basis to minimize our computational effort. A real space mesh equivalent to a plane wave cut-off of 100 Ryd is used for the evaluation of the Hartree and exchange–correlation energies. Owing to the large system size and the cubic scaling of the computational effort with system size, we implement the approximation by Harris [45], which is a non-self-consistent version of DFT based on the linearization of the Kohn–Sham equations. The eigenvalue equations are solved by full diagonalization of the Hamiltonian matrix.

We performed a constant volume MD simulation using the Nosé thermostat with a time step $\Delta t = 1.0$ fs. The simulation procedure consists of the following steps: (i) the temperature of the system is initially raised to 2500 K and is equilibrated for about 0.5 ps. (ii) The resulting system is then cooled down to 1000 K over a time period of 1 ps in steps. (iii) We then equilibrate the system at 1000 K for 0.5 ps. (iv) This is followed by cooling to 300 K over a time period of 1 ps. (v) The system is then further equilibrated at 300 K for 0.5 ps. (vi) Finally it is relaxed at 0 K to the nearest minimum using the conjugate gradient (CG) method until the maximum atomic force on each of the atoms is less than 0.03 eV Å$^{-1}$. These steps are then repeated for each of the candidate solutions mentioned in section 3.

## 5. Results and discussions

### 5.1. Local structure and bonding environment

We begin our discussion by focusing on the local structure and the bonding environment of the atoms via two- and three-body correlation functions. The correlation functions are calculated as radial and bond angle distributions providing information on the nature of short range order in the network. For this binary system, we have studied three partial radial distributions of the components: C–C, Si–C and Si–Si. Together with the reduced three-body correlation (i.e. the bond angle distribution), the local network properties can be studied and compared to the structural data from experiments. In figures 1(a)–(d), we present the normalized total and partial radial distribution functions (RDF). The Si–C first maximum peak in figure 1(b) is clearly seen at around 1.9 Å, which is in agreement with experiments [12, 9] and previous theoretical calculations [16, 17, 19–21, 23–25, 27]. Similarly, the C–C and Si–Si first maxima at 1.55 Å and 2.25 Å, respectively, are also in agreement with experimental data [9]. The total RDF in figure 1(a) clearly indicates a dominant Si–C peak implying the presence of strong chemical order in the network. A comparison of the peak heights of the C–Si and C–C from the partial RDFs suggests that the network is dominated by chemical order as far as the RDFs are concerned.

Further information about the local environment can be obtained by studying the coordination between Si and C atoms. For this purpose, we have used the location of the first minimum from the partial radial distributions as the cut-off distance to define the first coordination shells. In particular, the Si–C, C–C and Si–Si nearest neighbor cut-offs have been found to be $R_{\mathrm{Si–C}} = 2.25$ Å, $R_{\mathrm{C–C}} = 1.9$ Å and $R_{\mathrm{Si–Si}} = 2.5$ Å. The bond angles centered at the carbon and silicon atoms are also calculated using the same cut-off parameter. In figure 2, we plot the bond angle distributions for the C- and Si-centered angles along with the total bond angles. The average bond angle for the total distribution has been found

[3] Computer simulation of *a*-SiC starting with randomized diamond structure via the Wooten, Winer and Weaire (WWW) bond switching algorithm [35] has indicated that for a small degree of disorder the system has the tendency to get back to the crystalline structure after relaxation. This is avoided by making bond switches beyond a critical number in the WWW method, and by melting the initial structure in the 'quench-from-the-melt' approach. A choice of randomized *c*-SiC as a starting structure may therefore be an inappropriate one unless the crystalline memory of the structure is fully eliminated.

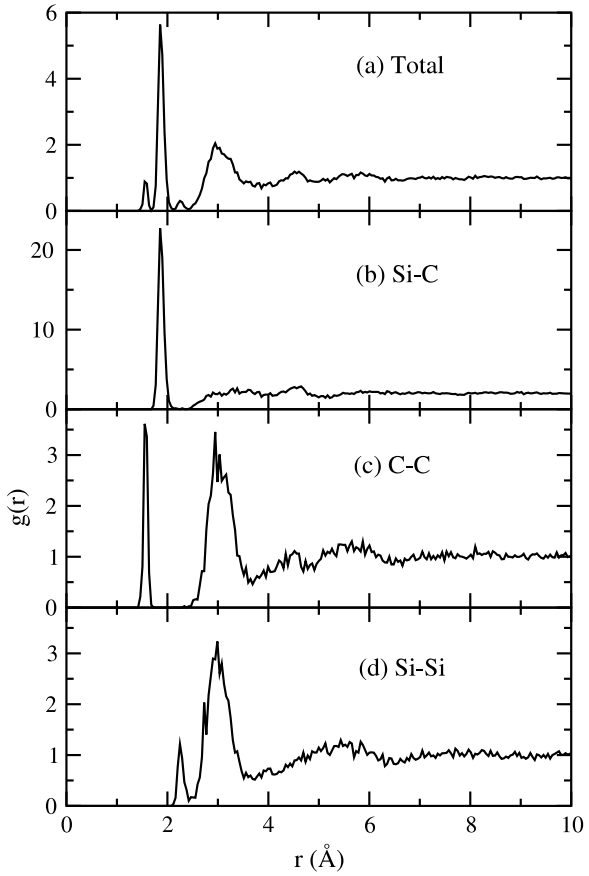


**Figure 1.** The total and partial radial distributions for the various pairs obtained from the model network. The distributions are all normalized for the purpose of comparison.

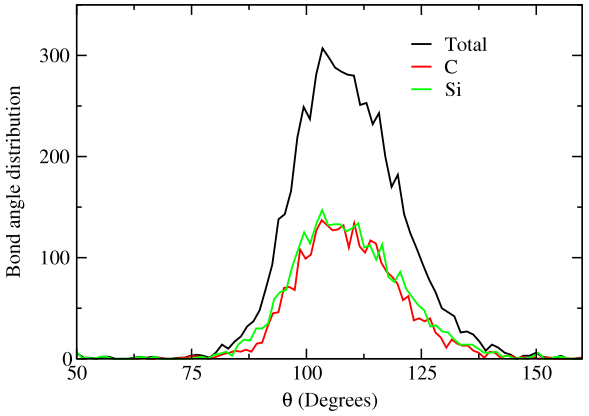


**Figure 2.** The bond angle distributions for the *a*-SiC network as discussed in the text. The distributions for angles centered at C and Si atoms are plotted along with the total bond angle distribution as indicated in the figure.

to be $\langle\theta\rangle = 109°$ with a root mean square (RMS) deviation of about $\Delta\theta = 12.1°$. The corresponding values for the partials are $\langle\theta\rangle_C = 109.2°$, $\Delta\theta_C = 11.3°$ and $\langle\theta\rangle_{Si} = 108.7°$, $\Delta\theta_{Si} = 12.9°$. These suggest that the final network continues to display tetrahedral character of its crystalline counterpart. Together with the short range chemical order

**Table 1.** Comparison of various structural parameters in this work and previous experimental and theoretical works. $\langle N_C\rangle$ and $\langle N_{Si}\rangle$ are the partial average coordination numbers of C and Si, respectively, while $\langle N\rangle$ is the total average coordination number. The chemical disorder parameter is denoted by $\chi = n_{CC}/n_{SiC}$, where $n_{CC}$ and $n_{SiC}$ are the percentage of C–C and Si–C bonds, respectively.

| | $\chi$ | $\langle N_C\rangle$ | $\langle N_{Si}\rangle$ | $\langle N\rangle$ |
|---|---|---|---|---|
| Present work | 0.083 | 3.98 | 4.01 | 4.00 |
| [12][a] | 0.00 | | | 3.99 |
| [16][b] | 0.6 | 3.85 | 3.93 | 3.89 |
| [17][b] | 0.5 | 3.46 | 4.02 | 3.74 |
| [19][b] | 0.50 | 4.00 | | |
| [20][b] | 0.60 | | | |
| [21][b,c] | 0.027 | 3.94 | 3.96 | 3.95 |
| [26][b] | 0.06–0.13 | | | |
| [27][b] | 0.00 | | | 3.79 |

[a] Experiment. [b] Theory. [c] Configuration labeled TB-216D in [21].

(manifested in the partial RDFs) and atomic coordination, the width of the bond angle distributions determine the overall quality of the network. A large value of the width $\Delta\theta$ is indicative of high degree of disorder that affects the electronic properties by introducing gap states in the electronic spectrum. Since electronic properties play an important role in structure evaluation, a comparison with the models in the literature would be relevant at this point. Devanathan *et al* [25] obtained values of $\Delta\theta_C = 16°$ and $\Delta\theta_{Si} = 36°$, whereas Rino *et al* [27] reported values of $\Delta\theta_C = 15°$ and $\Delta\theta_{Si} = 16°$.

A question of considerable importance, and somewhat controversial, is the extent of chemical disorder present in the amorphous SiC network. Unlike amorphous silicon where $sp^3$ hybridization is the mechanism of bond formation between the neighboring atoms, the carbon chemistry permits C atoms to bond via $sp^1$, $sp^2$ and $sp^3$ hybridization, making the local structure much more complex in a disordered environment. Following Tersoff [19], we define a short range order parameter $\chi$ as the ratio of the number of C–C and C–Si bonds present in the network. Denoting $n_{AB}$ (where A/B = Si, C) as the percentage of A–B bonding, we have found the values of C–C, Si–C and Si–Si bonding as 7.1%, 85.5% and 7.4%, respectively, and $\chi = 0.083$. Similarly, the percentage $C_k$ of atoms that are $k$-fold coordinated has been found to be 2.6% (3-fold), 95.3% (4-fold), 2.0% (5-fold) and 0.1% (6-fold), respectively. This shows that the total coordination defect concentration is only about 4.7%, implying a minor deviation from an ideal four-fold coordination. A comparison of the various structural parameters from the present study to some of the earlier studies is presented in table 1.

In order to get an idea about the topological connectivity of the network, the type and the number of rings present in the network are computed. The irreducible ring statistics for various $n$-member rings are computed and the results are reported in table 2. We define an irreducible ring as one that cannot be further partitioned into smaller rings. In other words, for a ring of size $n$, the minimum path starting from a given atom and to coming back to the same atom in an irreversible manner consists of $n$ hops. A six-member ring, which is the only ring in crystalline SiC (with ZnS structure), is dominant

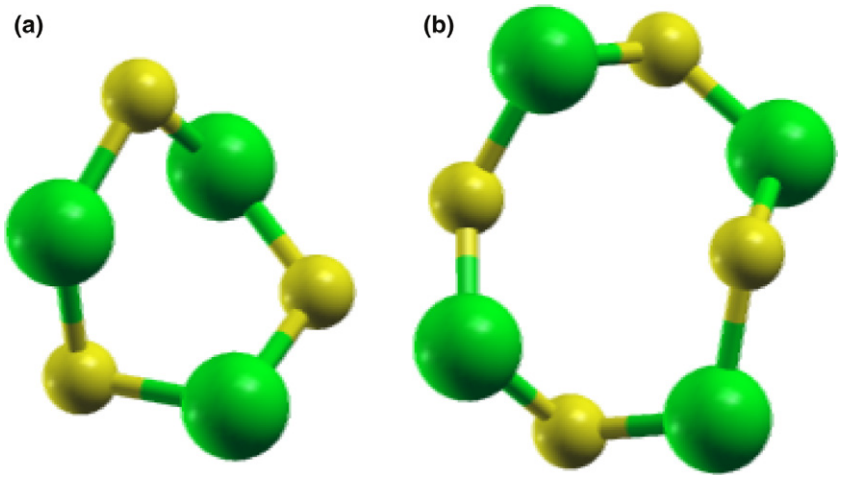


**Figure 3.** Representative six- and eight-member irreducible rings present in the network. The carbon and silicon atoms are shown in yellow (small) and green (large) respectively: (a) six-fold, (b) eight-fold.

**Table 2.** Irreducible ring statistics based on the nearest neighbor cut-off defined in the text.

| Ring size | 3 | 4 | 5 | 6 | 7 | 8 | 9 |
|---|---|---|---|---|---|---|---|
| Rings per atom | 0.002 | 0.015 | 0.432 | 0.749 | 0.495 | 0.146 | 0.040 |

in our network followed by seven- and five-member rings. This again implies the presence of tetrahedral character, as already observed via bond angle distribution. Owing to few homonuclear bonds, almost all the rings consist of alternating Si and C atoms. In figure 3, we have shown two representative six- and eight-member rings.

We summarize the structural properties by noting that (1) the network has small RMS width of the bond angle deviations compared to models in the literature, and (2) it has a small coordination defect. Together with these, the ring statistics further confirms that the network is not strained and, therefore, should have good electronic properties. The latter aspect of the model is addressed in section 5.2 of this paper. Furthermore, we have also noted, contrary to previous calculations [16, 17], that there is no graphene-like structure (three-fold coordinated carbon sheet with $\theta = 120°$) in the network. This is not surprising in view of the fact that our model has very few C–C wrong bonds.

### *5.2. Electronic properties*

While a great deal of information can be obtained from studying structural properties of the network via two- and three-body correlation functions and local coordination analysis, the electronic spectrum provides a more refined aspect of the local environment. In particular, the degree of local disorder is reflected in the local electronic density of states (l-EDOS) via formation of gap states and in the nature of the band tails of the spectrum. A high degree of local disorder causes the gap to appear narrow and noisy, which is difficult to gauge from only partial RDFs and the bond angle distribution. Partial coordination number analysis does provide some information on the nature of the electronic density of states (e.g. the presence of dangling bonds), but for a detailed understanding of electronic properties and the nature of the wavefunctions near the bandgap(s) one needs to calculate the electronic density of states (EDOS) of the model network. This is particularly important for models obtained via empirical potentials, but care must be taken in any approximate method to make sure that the EDOS is reasonably good and reflects the correct local chemistry. The electronic density of states for our model is obtained via diagonalization of the density functional Hamiltonian from SIESTA.

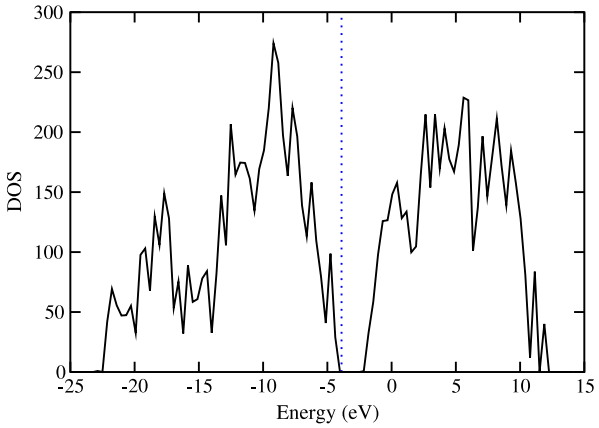


**Figure 4.** The electronic density of states for the *a*-SiC network obtained from the first-principles SIESTA Hamiltonian discussed in the text. The eigenvalues are broadened using a Gaussian width of 0.01 eV. The Fermi level is indicated as a dashed vertical line in the figure.

In figure 4 we present the Gaussian-broadened electronic density of states for the single particle Kohn–Sham energy eigenvalues. Several important observations are in order. First, the model shows the presence of a clean spectral gap. For a finite system, the gap size can be estimated as the difference between the highest occupied molecular orbital (HOMO) and the lowest unoccupied molecular orbital (LUMO). The exact value of the HOMO–LUMO gap for our model is found to

be 1 eV, which is about 1.2 eV smaller than the experimental bandgap for 3C-SiC of 2.2 eV [46]. However, as observed from figure 4, the average gap size is greater than 1 eV and is much closer to the experimental value taking into account some defect states that are close to the main conduction band. It is noteworthy that even though LDA underestimates the size of the gap, our model does produce an almost clean gap in the spectrum. This is a further indication that our method correctly identifies low-lying minima in the configuration space. We want to emphasize that this is an important aspect of our method, despite it being approximate in nature.

A further characterization of our model comes from the nature of the band tail states. In an amorphous system, one expects the band tails to show some signature of localization due to topological and chemical disorder in the network. This is independent of the presence of defects in the system. To study this, one often uses an ad hoc measure for eigenstate localization known as the *inverse participation ratio* (IPR). To put it simply, IPR approximately measures the *reciprocal* of the number of atoms that participate in localizing an eigenstate. While IPR is not the best way to quantify the degree of localization, it does provide some qualitative idea about the spread of an eigenstate over the atoms. For a multiband Hamiltonian, given a normalized eigenstate $\Psi$ with eigenenergies $E$, we first compute the Mulliken charge contribution from each atom as $q_i$ by projecting the eigenvector onto the orbitals centered on the atomic site $i$ and then sum over the orbitals to get the total contribution. The IPR can be expressed as

$$\mathrm{IPR}(E) = \sum_{i=1}^{N} q_i^2 = \sum_{i=1}^{N} \left( \sum_{j \in n_i} |\langle \phi_j | \Psi \rangle|^2 \right)^2 \qquad (2)$$

where $N$ is the total number of atoms, $i$ and $j$ are the site and orbital indices respectively, and $n_i$ is the number of basis orbitals at the site $i$. If the eigenstate $\Psi$ is completely localized, then only a single atom participates in localizing $\Psi$, yielding $\mathrm{IPR}(E) = 1$. Otherwise, if $\Psi$ is completely delocalized, then all the atoms participate equally in spreading $\Psi$, giving $q_i = 1/N$ and $\mathrm{IPR}(E) = 1/N$. Thus a large IPR value is generally attributed to localized states and vice versa. In figure 5 we plot the electronic IPR versus energy eigenvalue in the vicinity of the Fermi level. Each spike is located at an energy eigenvalue. The values of the IPR clearly show that the states near the bandgap are more localized than the states further away from the gap. A pictorial representation often helps us to better understand this behavior and is given in figure 6. To this end, we assign different colors to each site according to its Mulliken charge contribution to a given eigenstate. We then depict the spatial feature by showing a fraction (70%) of the total charge for the HOMO and LUMO states in the plot.

It is clear from figure 6 that the eigenfunctions (corresponding to HUMO and LUMO) are mostly confined to a small cluster of atoms in space. While the size of the cluster, to an extent, depends on the chosen fraction of Mulliken charge, it nonetheless confirms the localized nature of these two states in real space. For the highest occupied state, a silicon atom (large

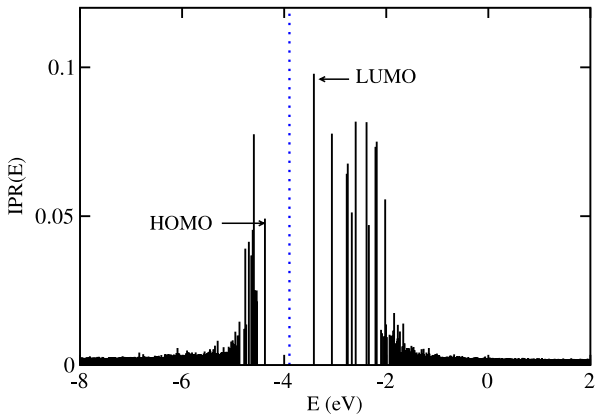


**Figure 5.** Inverse participation ratio (IPR) for the 1000-atom a-SiC model as a function of electronic eigenvalues. The highest occupied (HUMO) and the lowest unoccupied (LUMO) molecular orbitals are indicated in the figure. The large IPR values reflect the localized nature of the states in real space.

and colored red in the plot) has the largest contribution of about 14% of the unit charge. This atom is four-fold coordinated, and has two homonuclear and two heteronuclear bonds. For the LUMO state, the largest contribution to the Mulliken charge is about 25% and comes from a silicon atom (colored black). This atom is also four-fold coordinated with two homonuclear and two heteronuclear bonds.

### *5.3. Vibrational spectrum*

The vibrational density of states (v-DOS) of the model can be studied by computing the vibrational eigenmodes and eigenfrequencies. Since the energy associated with a typical vibrational degree of freedom is much lower than that of the electronic density of states, a slight deviation in the local geometry may cause a significant deviation in the vibrational spectrum and the modes of vibrations of the atoms. Such changes often can be difficult to observe in the electronic density of states, and therefore for a full characterization of the model one needs to ascertain the vibrational eigenmodes and the nature of vibrations. In this work, we address this issue by computing the modes via direct diagonalization of the dynamical matrix. Once the eigenmodes are available, the corresponding vibrational IPR can be calculated for each of the eigenfrequencies and the nature of the modes can be analyzed.

The dynamical matrix elements are constructed by successively displacing each atom in the fully optimized supercell along the positive and negative direction of the three orthogonal axes, and computing the resulting atomic forces within the harmonic approximation. Unlike the electronic IPR, we define here the vibrational IPR in a somewhat different way. Denoting a normalized vibrational eigenmode with frequency $\omega$ by $\mathbf{\Phi} = (\mathbf{\Phi}^1, \mathbf{\Phi}^2, \ldots, \mathbf{\Phi}^N)$, where $\mathbf{\Phi}^i = (\Phi^i_x, \Phi^i_y, \Phi^i_z)$ and $i$ is the atomic index, the IPR is defined as

$$\mathrm{IPR}(\omega) = \sum_{i=1}^{N} (\mathbf{\Phi}^i \cdot \mathbf{\Phi}^i)^2. \qquad (3)$$

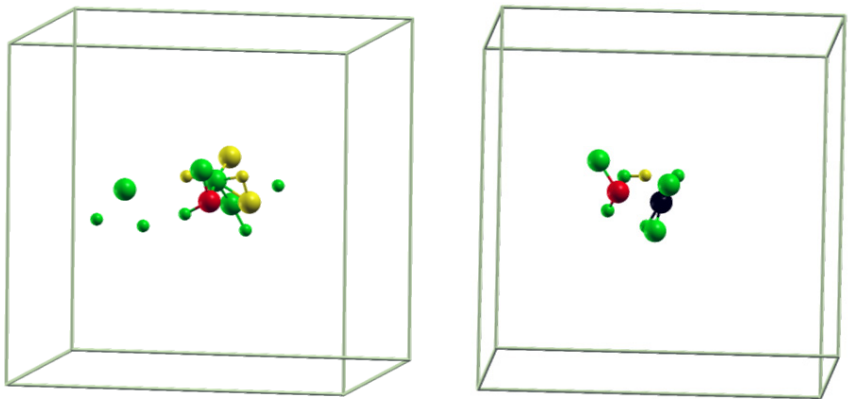

**Figure 6.** Spatial character of the localized HOMO (left) and LUMO (right) eigenstates. Silicon atoms are shown somewhat larger in the figure than the C atoms. The following color code is used to map the Mulliken charge $q$ for the states at each atomic site: black ($q > 0.20$), red or dark grey ($0.10 < q \leqslant 0.20$), gold or light grey ($0.05 < q \leqslant 0.10$) and green or grey ($0.01 < q \leqslant 0.05$). HOMO: $E = -4.38$ eV, IPR $= 0.05$; LUMO: $E = -3.42$ eV, IPR $= 0.098$. The color figures are available from the authors on request.

For an ideally localized $\mathbf{\Phi}$, only one atom contributes to the vibrational amplitude and so IPR$(\omega) = 1$. Similarly, for an ideally delocalized $\mathbf{\Phi}$, all atoms contribute uniformly to the amplitude, yielding IPR$(\omega) = 1/N$.

In figure 7 we show, in the upper panel, the plots for the atom-projected (weighted by the atomic contribution to the amplitude of the eigenstate conjugate to a given eigenfrequency) and total v-DOS. The corresponding vibrational IPR is plotted in the lower panel. The v-DOS clearly shows that the low frequency bands are dominated by Si while the high frequency bands mostly originate from the vibrations of C atoms. The overall shape and peak positions of the partial and the total v-DOS are in agreement with recent calculations by Vashishta *et al* [7] using an empirical potential. The IPR for the vibrational spectrum clearly distinguish two different type of modes: low frequency extended modes primarily arising from the Si atoms and the high frequency localized modes originating mostly from the C atoms. The nature of vibrations for a given frequency can be obtained by studying the corresponding eigenmode that gives the vibrational contribution coming from each of the atoms. The most localized vibrational mode appears at a frequency of 142 meV having an IPR value of 0.634. A real space mode analysis reveals that the vibration corresponds to a Si–C stretching mode with 78% of the mode confined on the C atom and about 12% on the Si atom, leaving behind the remaining 10% on the neighboring atoms. Similar analysis of the other localized states suggests all the high frequency states are localized and are centered on C atoms.

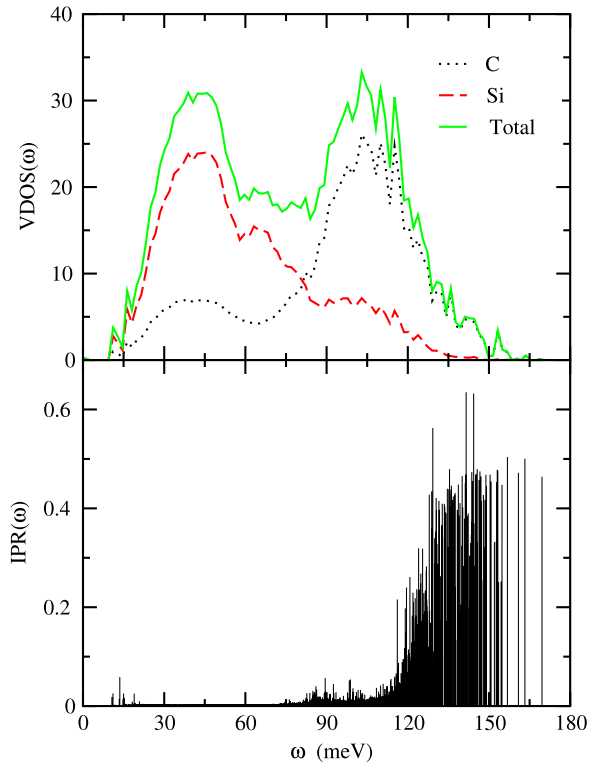


**Figure 7.** Atom-projected and total vibrational density of states (upper panel) and vibrational IPR (lower panel) for the 1000-atom $a$-SiC model. The majority of the high frequency vibrational modes are found to be localized on C atoms that form C–C and Si–C bonds.

## 6. Conclusion

We present an approximate first-principles molecular dynamics simulation of $a$-SiC within the density functional formalism coupled with *a priori* information obtained from experimental data. The method consists of generating a set of smart structural configurations as candidate solutions starting from a generic binary tetrahedral network and importance sampling of the solution subspace by incorporating characteristic structural, topological and experimental information in conjunction with an approximate first-principles force field to minimize the total energy in the desired solution space. Each of the samples is then used in our *ab initio* constant temperature molecular dynamics to find the minimum energy configuration, and the global minimum of this set is used as a final solution in our work. We have studied structural, electronic and vibrational properties for 50–50 $a$-SiC by using a localized basis first-principles molecular dynamics method. The degree

of chemical disorder, expressed as a ratio of the C–C to the Si–C bonds, is found to be approximately 0.083. The percentages of C–C, Si–C and Si–Si bonds in the network are observed to be 7.1%, 85.5% and 7.4%, respectively. The coordination defect concentration found in our model is low, at about 4.7%, while the average bond angle and its RMS width are about 109° and 12.1°, respectively. The electronic spectrum reveals a reasonably clean gap (HOMO–LUMO) of about 1 eV taking into account the defect states in the gap. Inverse participation ratio (IPR) analysis indicates that the HUMO and the LUMO are mostly localized on a four-fold coordinated atom having at least one wrong bond. The same observation applies to most of the band tail states as well. A similar analysis of the vibrational spectrum within the harmonic approximation suggests that the low frequency bands are dominated by Si vibrations whereas the C atoms mostly involve high frequency vibrational modes. A real space analysis of the high frequency vibrational modes (identified via IPR) shows that the vibrations are mostly stretching in character with larger contributions coming from the C atoms.

## Acknowledgments

The authors thank Normand Mousseau (University of Montreal) and Gerard Barkema (ITP, Utrecht) for providing binary continuous random networks that were used for smart structure generation. PB acknowledges the support of the University of Southern Mississippi under grant no. DE00945 and also thanks the Aubrey Keith Lucas and Ella Ginn Lucas Endowment for awarding a fellowship under the faculty excellence in research program.

## References

[1] Levinshteæin M E, Rumyantsev S L and Shur M 2001 *Properties of Advanced Semiconductor Materials: GaN, AlN, InN, BN, SiC, SiGe* (New York: Wiley)
[2] Emin D, Aselage T L and Wood C (ed) 1987 *Novel Refractory Semiconductors* (*Material Research Society Symp. Proc.* vol 97) (Pittsburg, PA: Material Research Society)
[3] Marshall R C, Faust J W and Ryan C E 1974 *Silicon Carbide-1973; Proc.* Air Force Cambridge Research Laboratories (US) and University of South Carolina, 1st edn (Columbia, SC: University of South Carolina Press)
[4] O'Connor J R and Smiltens 1960 *Silicon Carbide, A High Temperature Semiconductor; Proc.* Air Force Cambridge Research Laboratories (US) Electronic Research Directorate (Oxford: Pergamon)
[5] Pechenik A, Kalia R K and Vashishta P 1999 *Computer-Aided Design of High-Temperature Materials* (New York: Oxford University Press)
[6] Thorpe M F and Mitkova M I (ed) 1997 *Amorphous Insulators and Semiconductors* (*NATO Science Partnership Sub-Series 3* vol 23) (Berlin: Springer)
[7] Vashishta P, Kalia R K and Nakano A 2007 *J. Appl. Phys.* **101** 103515
[8] Gorman M and Solin S A 1974 *Solid State Commun.* **15** 761
[9] Ishimaru M, Bae I-T, Hirata A, Hirotsu Y, Valdex J A and Sickafu K E 2005 *Phys. Rev.* B **72** 024116
[10] Lee W Y 1980 *J. Appl. Phys.* **51** 3365
[11] Katayama Y, Usami K and Shimada T 1981 *Phil. Mag.* B **43** 283
[12] Kaloyeros A E, Rizk R B and Woodhouse J B 1988 *Phys. Rev.* B **78** 13099
[13] Bolse W 1999 *Nucl. Instrum. Methods* B **148** 83
[14] Ishimaru M, Bae I-T, Hirotsu Y, Matsumura S and Sickafu K E 2002 *Phys. Rev. Lett.* **89** 05502
[15] Snead L L and Zinkle S J 2002 *Nucl. Instrum. Methods* B **191** 497
[16] Finocchi F, Gali G, Parinello M and Bertoni C M 1992 *Phys. Rev. Lett.* **68** 3044
[17] Kelires P C 1992 *Phys. Rev.* B **46** 10048
[18] Tersoff J 1989 *Phys. Rev.* B **39** 5556
[19] Tersoff J 1994 *Phys. Rev.* B **49** 16349
[20] Mura D, Colombo L, Bertoncini R and Mula G 1998 *Phys. Rev.* B **58** 10357
[21] Ivashchenko V I, Turch P E A, Shevchenko V I, Ivashchenko L A and Rusakov G V 2002 *Phys. Rev.* B **66** 195201
[22] Gao F and Weber W J 2001 *J. Appl. Phys.* **89** 4275
[23] Malerba L and Perlado J M 2001 *J. Nucl. Mater.* **289** 57
[24] Yuan X and Hobbs L W 2002 *Nucl. Instrum. Methods* B **191** 74
[25] Devanathan R, Gao F and Weber W J 2007 *Nucl. Instrum. Methods* **255** 130
[26] Gao F and Weber W J 2002 *Nucl. Instrum. Methods* B **191** 504
[27] Rino J P, Ebbsjö I, Branicio P S, Kalia R K, Nakano A, Shimojo F and Vashishta P 2004 *Phys. Rev.* B **70** 045207
[28] Martin R 2004 *Electronic Structure: Basic Theory and Practical Methods* (Cambridge: Cambridge University Press)
[29] Hartmann A K and Rieger H 2002 *Optimization Algorithms in Physics* (Berlin: Wiley–VCH)
[30] Elliot S R 1990 *Physics of Amorphous Materials* (Essex: Longman Scientific & Technical)
Rao K J 2002 *Structural Chemistry of Glasses* (Oxford: Elsevier)
[31] Tafen D N and Drabold D A 2003 *Phys. Rev.* B **68** 165208
[32] Tafen D N and Drabold D A 2005 *Phys. Rev.* B **71** 054206
[33] Biswas P, Tafen D N and Drabold D A 2005 *Phys. Rev.* B **71** 054204
[34] Wales D 2003 *Energy Landscapes: Applications to Clusters, Biomolecules and Glasses* (Cambridge: Cambridge University Press)
[35] Wooten F, Winer K and Weaire D 1985 *Phys. Rev. Lett.* **54** 1392
[36] Barkema G T and Mousseau N 2000 *Phys. Rev.* B **62** 4985
[37] Mousseau N and Barkema G T 2004 *J. Phys.: Condens. Matter* **16** S5183
[38] Ordejón P, Artacho E and Soler J M 1996 *Phys. Rev.* B **53** 10441
[39] Sánchez-Portal D, Ordejón P, Artacho E and Soler J M 1997 *Int. J. Quantum Chem.* **65** 453
[40] Soler J M, Artacho E, Gale J D, Garcá A, Junquera J, Ordejón P and Sánchez-Portal D 2002 *J. Phys.: Condens. Matter* **14** 2745
[41] Perdew J P and Zunger A 1981 *Phys. Rev.* B **23** 5048
[42] Troullier N and Martins J L 1993 *Phys. Rev.* B **43** 1993
[43] Kleinman L and Bylander D M 1982 *Phys. Rev. Lett.* **48** 1425
[44] Sankey O F and Niklewski D J 1989 *Phys. Rev.* B **40** 3979
[45] Harris J 1985 *Phys. Rev.* B **31** 1770
[46] See for example, the review article by Morkoc H, Strite S, Gao G B, Lin M E, Sverdlov B and Burns M 1994 *J. Appl. Phys.* **76** 1363